

Uncertainty Analysis for Hybrid Electric Propulsion in NASA EPFD Vehicles*

1st Tavish Pattanayak

*Daniel Guggenheim Department of Aerospace Engineering
Georgia Institute of Technology
Atlanta, USA
tpattanayak3@gatech.edu*

2nd Jaylon Uzodinma

*Daniel Guggenheim Department of Aerospace Engineering
Georgia Institute of Technology
Atlanta, USA
juzodinma3@gatech.edu*

3rd Raphael Gautier

*Daniel Guggenheim Department of Aerospace Engineering
Georgia Institute of Technology
Atlanta, USA
raphael.gautier@gatech.edu*

4th Turab Zaidi

*Daniel Guggenheim Department of Aerospace Engineering
Georgia Institute of Technology
Atlanta, USA
turab@gatech.edu*

5th Dimitri Mavris

*Daniel Guggenheim Department of Aerospace Engineering
Georgia Institute of Technology
Atlanta, USA
dimitri.mavris@aerospace.gatech.edu*

Abstract—The National Aeronautics and Space Administration (NASA)’s Electrified Powertrain Flight Demonstration (EPFD) program aims to advance hybrid-electric propulsion (HEP) as part of the aviation industry’s decarbonization efforts. However, the feasibility and performance of hybrid-electric aircraft are highly dependent on the development of key electrical components such as batteries, electric machines, and power converters, whose future capabilities remain uncertain. This paper presents an uncertainty quantification analysis of two hybrid-electric aircraft architectures: a turboprop aircraft and a turbofan aircraft. Using our established uncertainty propagation framework, we assess the impact of technological uncertainty on the design and performance of both vehicle configurations. The turboprop vehicle analysis builds on prior work, incorporating the latest iteration of the vehicle model, which was a retrofit study, while the turbofan analysis extends the framework to a revised model - incorporating an updated thermal management system along with a new operational mode for electric taxiing. The results indicate that hybridization offers promising benefits for the turboprop vehicle, whereas the potential advantages for the turbofan architecture appear less optimistic. The results indicate that hybridization offers promising benefits for the turboprop vehicle, whereas the potential advantages for the turbofan architecture appear less optimistic. These findings highlight the importance of tailored hybrid-electric strategies and demonstrate the utility of uncertainty quantification in guiding technology-informed design decisions.

Index Terms—Hybrid-Electric Propulsion, Uncertainty Quantification, Turboprop, Turbofan, Electrified Aircraft, Sustainable Aviation

NASA Grant - 80LAR23DA003

I. INTRODUCTION

A. Motivation

The aviation industry currently emits more than 900 million tons of CO₂ annually, accounting for approximately 2 to 2.5% of total global CO₂ emissions. With growing air travel demand, its environmental impact will rise without effective mitigation. To counter this, the International Civil Aviation Organization (ICAO) targets net-zero aviation emissions by 2050. In the near term, hybrid-electric propulsion (HEP) is a promising transitional solution that balances electrification benefits with current technological limitations of key electrical powertrain components. Thus, the NASA Electrified Powertrain Flight Demonstrator (EPFD) program aims to advance the maturation of hybrid-electric propulsion (HEP) technologies through demonstration and development efforts, helping to pave the way for more sustainable aviation solutions.

B. Background

This paper builds upon prior work in [1], [2], [3], and [4], to provide updated uncertainty quantification results for both hybrid-electric turboprop and turbofan vehicle models. A significant change affecting the results in this paper is the adoption of updated technological projections from [5], which in some cases differ from those used in prior studies published [6], [7], and [8]. Additionally, the underlying models have been improved to provide more realistic and informative results. For the turboprop vehicle, the results for the retrofit vehicle model are being published for the first time. The modeling updates for the turboprop have been comprehensively discussed in the

[9] publication from the modeling team, however, high-level information is provided in this paper to make it as contained as possible. For the turbofan vehicle, the latest model has an enhanced thermal management system model as well as a new operational mode for taxiing.

1) *Uncertainty Quantification Framework*: The framework and setup used to perform uncertainty quantification in this work remains unchanged from [3]. The main assessment used to perform uncertainty quantification is referred to as the deterministic design optimization approach. This approach conducts design optimization and uncertainty propagation as distinct processes, with technological variables remaining fixed throughout the optimization. It is important to note that while design and operational constraints are applied during the initial deterministic design optimization, they are not enforced during uncertainty propagation. As a result, the final output distributions may include designs that violate these constraints. The method has been described in detail in [3].

To execute uncertainty quantification, surrogate models—which approximate the relationships between the inputs and outputs of the vehicle model—are employed in place of the full vehicle model. This substitution is necessary because directly integrating high-fidelity vehicle models into the uncertainty quantification workflow is computationally impractical due to its complexity and evaluation cost. To generate training data for surrogate models, two design of experiments (DoE) are created, which improves the accuracy of the uncertainty quantification (UQ) results. In DoE #1, technological variables are fixed to their most likely values, and design variables are varied so that we can create surrogates tailored to the initial deterministic design optimization phase. Next, for DoE #2, design variables are fixed to optimum values found using the previous DoE, and technological variables are varied in order to generate surrogates that can be then used for uncertainty propagation (UP). The subset of the data used to train the model comprised 80% of the evaluations. The remaining 20% are used for validation of the model after training. The validation data serves as an independent measure of how well the model generalizes to new data. A multi-layer perceptron (MLP) neural network was employed for the surrogate models, with different architectures and optimization techniques explored to find the best-performing models.

2) *Characterization of Technological Uncertainty*: In previous work, technological uncertainty was characterized using projections from [6], [7], and [8], which together project the future performance of key electrical components of a hybrid-electric powertrain. In each of these references, technological projections are defined with conservative, nominal, and aggressive values, which represent varying levels of optimism for future technological progress. The conservative, nominal, and aggressive values in technological projections are translated as the lower bound, peak, and upper bound of triangular probability distributions, respectively. Pack factor and high-pressure compressor efficiency Δ are used only for the turbofan. Since the projections for these variables only feature lower and upper bounds, these variables are characterized by uniform

TABLE I: Comparison of the previously used conservative (cons.), nominal (nom.), and aggressive (agg.) projections of uncertain technological parameters with the current values used in this paper.

Parameter	Projections	Cons.	Nom.	Agg.
Battery cell-level specific energy (Wh/kg)	Previous	359	489	584
	Current	357	378	444
Electric machine specific power (kW/kg)	Previous	9.2	13.2	16.1
	Current	5	10	15
Electric machine efficiency (%)	Previous	96.3	96.8	97.4
	Current	92	94	95
Power converter specific power (kW/kg)	Previous	9.6	13.8	17.3
	Current	8	12	20
Power converter efficiency (%)	Previous	98.2	98.5	98.8
	Current	97	99	99.5
*Pack factor	Previous	0.4	0.4	1.0
	Current	0.4	0.4	1.0
*High pressure compressor efficiency Δ	Previous	0.003	0.01	0.023
	Current	0.003	0.01	0.023

* Indicates the variable is only used for the turbofan vehicle

distributions rather than triangular distributions.

The technological projections used in previous studies and in work documented in this paper are shown in Section I-B2. The projections are similar but have slight differences for some variables. Specifically, the projections used in this paper reflect less optimism for technological progress for batteries and electric machines in the near term. For power converters, the projected technological progress has a wider range in the new projections compared to that of the old projections. It is important to note that for all technological variables, the latest projections include values outside of the ranges in the previous projections, which indicates a need to create an updated DoE for surrogate model training in order to avoid extrapolating variable relationships beyond the domain for which the initial surrogate models were trained. Compared to previous work, the variable ranges are wider for some technological inputs, so the total number of DoE samples was increased from 10,000 to 12,000 to ensure sufficient sampling density across the input variable space while also accounting for failed cases, if any.

3) *Mathematical Formulation of the UQ Approach*: In the deterministic design optimization approach that we introduced previously, technological variables are fixed throughout the optimization, and design optimization is performed deterministically. Constraints are applied during the optimization, but they are not enforced during uncertainty propagation, which occurs as a separate step.

Formulation:

- Fix: Technological variables x_t to x_t^{nom} .
- Minimize: Objective function $f(x_d, x_t^{nom})$
- With respect to: Design variables x_d
- Subject to:
 - Constraints on the design variables' ranges: $x_{d_{min}} \leq$

$$x_d \leq x_{d_{max}}$$

– Other constraints: $c_i(x_d, x_t^{nom.}) \leq 0$

Note: After this optimization, uncertainty propagation (e.g., via Monte Carlo sampling) may be performed separately, but the resulting output distributions may include designs that violate $c(x_d, x_t^{nom.}) \leq 0$.

II. TURBOPROP ARCHITECTURE

A. Model Updates

The current literature review highlighted the advantages of hybrid propulsion in aircraft through comprehensive redesign and optimization using projected future technologies [10]. However, in the near term, converting existing aircraft to hybrid propulsion may be more economically feasible by reducing development expenses. Depending on the hybridization level, these retrofits could enhance fuel efficiency on shorter flights, though potentially at the cost of decreased range due to battery energy density limitations. The previous model, referenced in [1], analyzed a hybrid-electric turboprop configuration based on an earlier iteration of the vehicle architecture. The updated model in this paper is based on the parametric mission performance assessment conducted in [9], which specifically evaluates the retrofitting of the DHC-7-102, which utilizes a four-engine configuration with hybrid-electric propulsion as part of NASA’s Electrified Powertrain Flight Demonstration (EPFD) program.

A key distinction between the models lies in their approach to vehicle design. The previous model assumed a clean-sheet hybrid-electric aircraft, whereas the updated model explores hybridization as a retrofit to the existing DHC-7 airframe. This approach maintains the fundamental aircraft structure while optimizing the integration of hybrid-electric propulsion components, providing a more realistic near-term pathway for implementation. It also integrates updated technological projections from [5], which replace earlier projections from [6], [7], and [8]. These refinements contribute to improved fidelity in performance estimation, particularly for the 2030 operational timeframe.

B. Optimization Setup

1) *Design Variables:* The primary design variables are:

- **Motor Power Split:** Fraction of total shaft power provided by electric motors during takeoff, ranging from 10% to 40%.
- **Climb Motor Power Code:** Output of electric motors as a percentage of their rated power, ranging from 80% to 100%.
- **Fixed Battery Duration:** Available battery duration, ranging from 0.5 to 1.4 hours.

2) *Technological Variables:* The technological parameters that influence the performance of the electric powertrain are modeled as either fixed values for deterministic optimization or probabilistic distributions for uncertainty quantification. These are shown in the Section I-B2.

3) *Constraints:* The optimization aims to minimize both block fuel consumption and total block energy usage subject to the constraints given in the Table VI.

TABLE II: Optimization Constraints for Turboprop Vehicle

Constraint	Operator	Limit	Units
Taxi Thrust-to-Weight Ratio	\geq	0.03	–
Time to Climb	\leq	19.1	mins
Rate of Climb at TOC	\leq	300	ft/min
Maximum Specific Excess Power (Primary)	\leq	0	ft/min
Maximum Specific Excess Power (Reserve)	\geq	0	ft/min
Ramp Weight	\leq	20,003.5	kg
Feasibility of energy source - Fuel	\leq	0	–
Feasibility of energy source - Battery	\leq	10^{-3}	–

4) *Baseline Vehicle Performance:* For comparison, the baseline DHC-7 aircraft was sized for a notional 600 nautical mile (nmi) mission. This aircraft has a block fuel consumption of 751.3 kg for the evaluated 200 nmi mission, and this value is used to calculate a percentage change in Block Fuel for the vehicle, henceforth denoted by Δ Block Fuel.

C. Results

1) *Surrogate Models:* All validation metrics were computed on a validation set - model observations not used for training the surrogate models. Design Mission refers to the original mission for which the baseline aircraft was designed, while Scatter Mission 2 refers to the off-design mission with a range of 200 nmi. For the optimization objective and constraints, an assessment of surrogate model fits based on the vehicle model data from DoE #1 is provided in Table III. These surrogate models approximate the relationships between the design inputs and the outputs and are then used to perform deterministic design optimization in order to find a fixed design point to propagate technological uncertainty.

TABLE III: Validation metrics for turboprop surrogate models

Output	R^2	RMSE	MAE
Maximum Specific Excess Power (Primary)	0.999	0.377	0.287
Maximum Specific Excess Power (Reserve)	0.999	2.775	2.315
Rate of Climb at TOC	0.999	0.456	0.348
Time to Climb	1.000	0.006	0.004
Taxi Thrust-to-Weight Ratio	0.998	0.004	0.003
Block Fuel	0.999	1.060	0.763
Feasibility of energy source - Fuel	0.999	0.002	0.001
Feasibility of energy source - Battery	0.937	0.019	0.012
Ramp Weight	1.000	15.329	11.525

Table III presents the relevant validation metrics, including coefficient of determination (R^2), root-mean-square error (RMSE), and mean absolute error (MAE). R^2 indicates the proportion of the surrogate error’s variance relative to the total

response variance. RMSE and MAE provide error estimates in the original response scale, with MAE representing the average surrogate error and RMSE capturing the spread of error, considering larger deviations more significantly. It can be observed in the validation set that the R^2 values are 1 or almost 1 for all variables with no outliers visible. For brevity, only validation metrics are presented here. The magnitude of error in the residual vs predicted values for all variables can be seen to be minimal.

2) *Uncertainty Quantification*: Using the optimal design and operational input values identified through optimization, uncertainty propagation in the technological variables listed in Section I-B2 was carried out using the surrogate models described earlier. Figure 1 shows the probability density and cumulative distribution of Δ Block Fuel as predicted by the deterministic design optimization process for the single objective optimization problem where the aim is to minimize block fuel. A negative sign indicates that all the samples in the analysis of the model show a reduction in the usage of fuel compared to the baseline, conventional vehicle. Δ Block Fuel is predicted to reduce by a mean of about 21%.

TABLE IV: Optimized Design Inputs for Turboprop

Design Input	Optimum	Units
Motor Power Split	0.154	%
Climb Motor Power Code	98.716	%
Fixed Battery Duration	0.864	hr

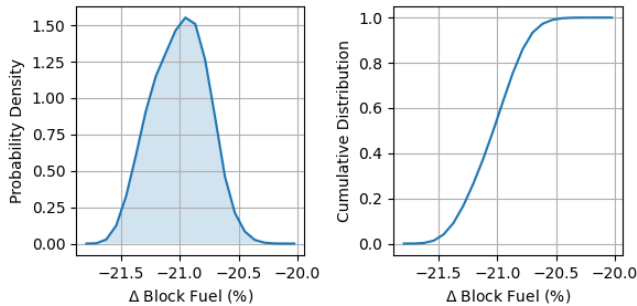


Fig. 1: Probability density and cumulative distribution of Δ Block Fuel as predicted by UP

TABLE V: Summary Statistics from UP using Turboprop Vehicle Model

Mean	Std. Dev.	5th Perc.	Median	95th Perc.
-21.00	0.24	-21.39	-21.00	-20.62

III. TURBOFAN ARCHITECTURE

A. Model Updates

The underlying vehicle model on which the results in this paper are based is a 150-passenger, narrowbody aircraft featuring a mild parallel hybrid electric powertrain. The baseline

for the powertrain is the Pratt & Whitney 1127G, which is the geared turbofan engine option available for the Airbus A320neo. For the hybrid electric powertrain model used in this study, both the low-pressure and high-pressure spools are augmented by separate electric machines. Previously, the powertrain model had five modes of operation: electric fan taxi, takeoff and climb boost, engine power extraction, sub-idle descent, and turbine electrified energy management. The various operational modes provide adaptability to different operational scenarios and contribute to the overall efficiency of the system. A key addition to the updated model in this work is the inclusion of wheel taxiing, which serves as an alternative to electric fan taxiing. Wheel taxi involves the use of battery-powered electric motors to drive the wheels of the hybrid-electric aircraft during taxi operations at an airport, and the results included in this work are specific to the wheel taxi option of the updated vehicle model. In order to maximize the benefits of changes to the powertrain, the vehicle's geometric parameters are considered variables that can be optimized according to defined objectives and constraints. Design and sizing of the aircraft are carried out in the Environmental Design Space (EDS) modeling environment, a physics-based aircraft modeling tool [11]. It is important to note that the aircraft is sized for a notional mission range of 3,420 nmi.

B. Optimization Setup

1) *Design Variables*: The primary design variables are:

- **Thrust-to-Weight Ratio**: The ratio of vehicle thrust to its weight, ranging from 0.28 to 0.36.
- **Wing Loading**: The ratio of the vehicle's weight to its wing area, ranging from 115 to 140 lb/ft².
- **Taper Ratio**: The ratio of the wing's tip chord to its root chord, ranging from 0.195 to 0.3132.
- **Thickness-to-Chord**: Ratio of the maximum vertical thickness of the wing relative to the chord, ranging from 0.09 to 0.13.
- **T_{4,max}**: Maximum turbine inlet temperature, ranging from 2,900 to 3,600 °F.
- **T_{4,margin}**: Difference in turbine inlet temperature between maximum takeoff thrust and maximum continuous thrust, ranging from -250 to -125 °F.
- **Wing Sweep**: The angle at which the wing is swept backward or forward, ranging from 19.5° to 29.93°.
- **Fan Pressure Ratio**: The ratio of the total pressure at the fan exit to the total pressure at the fan inlet, ranging from 1.35 to 1.55.
- **Operating Pressure Ratio at the Top of Climb**: The ratio of total pressure at the compressor exit to inlet at the top of the climb, ranging from 45 to 65.
- **High-Pressure Compressor Pressure Ratio**: The total pressure ratio between the high-pressure compressor exit and inlet, ranging from 13 to 20.
- **Extraction Ratio**: The proportion of engine airflow diverted from the engine to be applied to auxiliary functions, ranging from 0.9 to 1.35.

TABLE VI: Optimization Constraints for Turbofan Vehicle

Constraint	Operator	Limit	Units
Landing Approach Speed	\leq	140	kts
Wingspan	\leq	122	ft
Core Size	\leq	2.9	lbm/s
High-Pressure Compressor Exit Temperature	\leq	1,760	R
Fan Diameter	\leq	81.3	in
Excess Fuel	\leq	1,225	kg
2nd Segment Climb Thrust (One Engine Out)	\geq	0	lb
Takeoff Field Length (All Engines)	\leq	6,950	ft
Takeoff Field Length (One Engine Out)	\leq	8,000	ft
Climb Time	\leq	20	min

- **Power Shave Fraction:** Reduction of engine core size relative to baseline, ranging from 0.05 to 1.00.
- **Electrical Voltage:** Design voltage of the battery stack, ranging from 500 to 1,500 V.
- **Battery k8:** Technology factor on the maximum continuous current of the battery, ranging from 1.00 to 3.00.
- **Climb Rate Floor:** Floor climb rate that determines when a boost is necessary, ranging from 500 to 3,000 ft/min.

2) *Technological Variables:* The technological parameters that influence the performance of the powertrain for a hybrid-electric turbofan vehicle are modeled as fixed values for deterministic optimization, and these fixed values correspond to technological performance projections for the year 2030 as shown in the Section I-B2.

3) *Constraints:* The optimization aims to minimize block fuel consumption on a 900 nmi mission and is subject to the constraints in Table VI.

4) *Baseline Vehicle Performance:* For comparison, a non-hybrid turbofan vehicle model, also sized for a notional 3,420 nmi mission, was used as a baseline aircraft. This aircraft has a block fuel consumption of 3,461 kg for the evaluated 900 mission, and this value is used to calculate a percentage change in Block Fuel (900 nmi) for the hybrid-electric vehicle.

C. Results

1) *Surrogate Modeling:* For the optimization objective and constraints, an assessment of surrogate model fits based on EDS model data from DoE #1 is provided in Table VII. These surrogate models approximate the relationships between the design inputs (Section III-B1) and the outputs (Table VII), and these surrogate models will be used to perform deterministic design optimization in order to find a fixed design point to propagate technological uncertainty about. Thus, the quality of these surrogate model fits is key to establishing confidence in the design optimization results presented in this work. Similar to the turboprop vehicle model, the R^2 values calculated from the validation data are almost 1 for all outputs, and the magnitude of error in the residual vs predicted values for all outputs is acceptable for the described use case.

TABLE VII: Validation metrics for turbofan surrogate models

Output	R^2	RMSE	MAE
Block Fuel (900 nmi)	0.990	27.042	20.876
Landing Approach Speed	0.999	0.039	0.032
Wingspan	0.998	0.185	0.144
Core Size	0.999	0.018	0.013
High-Pressure Compressor Exit Temperature	0.999	1.341	1.035
Fan Diameter	0.999	0.207	0.161
Excess Fuel	0.999	144.890	108.150
2nd Segment Climb Thrust (One Engine Out)	0.974	252.004	131.275
Takeoff Field Length (All Engines)	0.984	82.818	45.165
Takeoff Field Length (One Engine Out)	0.984	114.754	58.625
Climb Time	0.981	0.380	0.277

After finding the optimum design point, additional EDS model data was generated for DoE #2, which only considers the varied technological inputs from Section I-B2. The model data from DoE #2 is used for uncertainty propagation, and specific focus is given to creating a quality surrogate model fit for block fuel on a 900 nmi mission, which is the key performance metric of comparison for the turbofan vehicle. The R^2 , RMSE, and MAE of the surrogate model for Block Fuel (900 nmi) are 0.988, 3.802, and 2.896, respectively.

2) *Uncertainty Quantification:* Using the surrogate models documented in Table VII, we found the following optimized values for the turbofan vehicle's design inputs. As mentioned, the current version of the turbofan vehicle has a new electric taxi operating mode called wheel taxi, and the design optimization results in Table VIII are specific to this electric taxi operational mode. A key finding in the current design optimization results is that the optimal power shave fraction is found to be 5%, which is its lower bound within DoE #1. This finding reinforces the challenges associated with applying electrification to vehicles in the 150-passenger size class since the optimizer minimizes the extent to which the gas turbine core is downsized as a byproduct of supplementary electric power provided by batteries and electric motors. However, even with a minimal core downsizing, fuel savings can still be obtained with sufficient performance of electrical components in the powertrain, which is the focus of the uncertainty propagation results.

After propagating technological uncertainty from the inputs in Section I-B2 to vehicle-level performance metrics, the resulting probability density and cumulative distribution are shown in Figure 2, and we observe that the entire distribution lies below 0%, which shows that incorporating wheel taxi with the technological projections from [5] yields hybrid-electric vehicle designs with superior fuel-burn performance compared to a future, non-hybrid vehicle. The distribution of Δ Block Fuel 900 has a mean of -2.58% and a standard deviation of

TABLE VIII: Optimized Design Inputs for Turbofan Vehicle

Design Input	Optimum	Units
Thrust-to-Weight Ratio	0.30	–
Wing Loading	115	lb/ft ²
Taper Ratio	0.195	–
Thickness-to-Chord	0.09	–
$T_{4,max}$	3,194	°F
$T_{4,margin}$	-186	°F
Wing Sweep	19.5	°
Fan Pressure Ratio	1.39	–
Operating Pressure Ratio at Top of Climb	57.0	–
High-Pressure Compressor Pressure Ratio	14.0	–
Extraction Ratio	1.09	–
Power Shave Fraction	5	%
Electrical Voltage	850	V
Battery k8	2,545	ft/min
Climb Rate Floor	1.00	–

0.42, which reflects optimism in the potential for electrification to reduce fuel burn for a 150-passenger, turbofan vehicle along a typical mission range. Sensitivity analysis indicates that high pressure compressor efficiency Δ is responsible for over 80% of the variability in Δ Block Fuel 900. Since this input is uniformly distributed and its impact does not exhibit strong nonlinearities, the resulting distribution lacks a distinct peak.

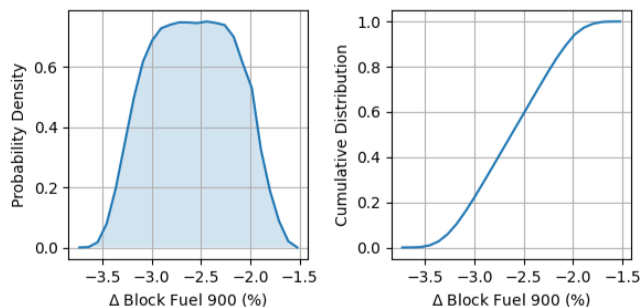


Fig. 2: Probability density and cumulative distribution of Δ Block Fuel 900 as predicted by UP

TABLE IX: Summary Statistics from UP using Turbofan Vehicle Model

Mean	Std. Dev.	5th Perc.	Median	95th Perc.
-2.58	0.42	-3.25	-2.58	-1.92

IV. CONCLUSION

This study presents an updated UQ analysis of HEP applied to two NASA EPFD vehicle architectures: a retrofitted turboprop and a redesigned turbofan. The results demonstrate the varying degrees of benefit that hybridization can offer depending on the vehicle type and the underlying technological assumptions. For the turboprop vehicle, the analysis highlights strong potential for fuel savings, with an average

block fuel reduction of approximately 21%. These results affirm the viability of hybrid retrofits for regional aircraft, particularly for short-range missions where battery limitations are less constraining. The updated modeling, based on a DHC-7 retrofit and current technological projections, provides a more grounded, near-term path toward electrified flight.

In contrast, the turbofan architecture—despite incorporating novel features such as wheel taxi and advanced thermal management—shows more modest benefits, with a mean fuel burn reduction near 2.5%. This reflects the inherent challenges of applying hybridization to larger, longer-range commercial aircraft, where the energy density of current battery technology remains a key limiting factor. Nevertheless, even minimal levels of electric augmentation, when strategically integrated, can contribute to performance gains under optimistic technological advancements.

Overall, the findings underscore the importance of tailored hybrid-electric strategies that consider vehicle class, mission profile, and realistic technology roadmaps. The UQ framework employed in this work proves effective in capturing the probabilistic nature of future HEP systems and provides valuable guidance for design decisions under uncertainty.

REFERENCES

- [1] Tavish Pattanayak, Jaylon Uzodinma, Raphael H. Gautier, Miguel Walter, Turab Zaidi, and Dimitri Mavris. Uncertainty analysis of turbofan and turboprop architectures for hybrid electric propulsion in nasa epfd vehicles. In *AIAA AVIATION FORUM AND ASCEND 2024*, 2024.
- [2] J. Uzodinma, T. Zaidi, M. Walter, and D. Mavris. Uncertainty quantification on a parallel hybrid-electric propulsion epfd vehicle. In *AIAA SciTech Forum*, National Harbor, MD, Jan, 2023.
- [3] R. Gautier, L. Teta, J. Uzodinma, T. Pattanayak, M. Walter, T. Zaidi, and D. Mavris. Impact of technological uncertainty on design parameter selection of the nasa parallel hybrid-electric propulsion epfd vehicle. In *AIAA AVIATION 2023 Forum*, 2023.
- [4] M. Walter, J. Uzodinma, T. Zaidi, R. Gautier, L. Teta, and D. Mavris. Sensitivity analysis within the benefit region of the nasa parallel hybrid-electric propulsion epfd vehicle. In *IEEE-AIAA ITEC-EATS 2023 Forum, Institute of Electrical and Electronics Engineers*, 2023.
- [5] Dahlia Pham, Carl Recine, and Ralph Jansen. Advanced turboprop transport aircraft modeling for the electrified powertrain flight demonstration project. *34th Congress of the International Council of the Aeronautical Sciences*, 2024.
- [6] Blake Tiede, Cody O’Meara, and Ralph Jansen. Battery key performance projections based on historical trends and chemistries. In *2022 IEEE Transportation Electrification Conference & Expo (ITEC)*, pages 754–759, 2022.
- [7] Chrysoula Pastra, Christopher Hall, Gokcin Cinar, Jon Gladin, and Dimitri Mavris. Specific power and efficiency projections of electric machines and circuit protection exploration for aircraft applications. pages 766–771, 06 2022.
- [8] C. Hall, C. L. Pastra, A. Burrell, J. Gladin, and D. Mavris. Projecting power converter specific power through 2050 for aerospace applications. In *IEEE-AIAA ITEC-EATS 2022 Forum, Institute of Electrical and Electronics Engineers*, 2022.
- [9] Yu Cai, Jiacheng Xie, Chrysoula L Pastra, Ngefor R Ndifor, Alexander M Kehler, and Dimitri Mavris. Parametric mission performance assessment of regional turboprop aircraft retrofitted with hybrid electric propulsion. In *AIAA AVIATION FORUM AND ASCEND 2024*, page 4038, 2024.
- [10] Yu Cai, Jiacheng Xie, Joshua Brooks, Jonathan Gladin, and Dimitri Mavris. System-level design space exploration of a parallel hybrid propulsion system for a regional short takeoff and landing turboprop aircraft. 06 2023.
- [11] Luis Salas Nunez, Jimmy C. Tai, and Dimitri N. Mavris. The environmental design space: Modeling and performance updates. *AIAA Scitech 2021 Forum*, 2020.